A&A 393, 1053–1064 (2002)
DOI: 10.1051/0004-6361:20020673

Astronomy & Astrophysics

Observations at Nançay of the OH 18-cm lines in comets

The data base. Observations made from 1982 to 1999⋆

J. Crovisier, P. Colom, E. Gérard, D. Bockelée-Morvan, and G. Bourgois⋆⋆

Observatoire de Paris-Meudon, 92195 Meudon, France

Received 9 November 2001 / Accepted 16 April 2002

Abstract. Since the apparition of comet Kohoutek 1973 XII, the 18-cm lines of the OH radical have been systematically observed in a number of comets with the Nançay radio telescope. Between 1973 and 1999, 52 comets have been successfully detected. This allowed an evaluation of the cometary water production rates and their evolution with time, as well as a study of several physical processes such as the excitation mechanisms of the OH radio lines, the expansion of cometary atmospheres, their anisotropy in relation to non-gravitational forces, and the Zeeman effect in relation to the cometary magnetic field. Part of these observations and their analysis have already been published. The bulk of the results are now organized in a data base. The present paper is a general presentation of the Nançay cometary data base and a more specific description of the observations of 53 cometary apparitions between 1982 and 1999. Comets observed before 1982 are only partly incorporated in the data base. Observations of comets since 2000 have benefited from a major upgrade of the telescope; they will be presented in forthcoming publications.

Key words. comets: general – radio lines: solar system – solar system: general

1. Introduction

A new era in the study of comets began in 1973 with the observations of the 18-cm lines of the OH radical, first detected in comet Kohoutek 1973 XII[1] (Biraud et al. 1974; Turner 1974). This discovery initiated a long-term programme of observation at the Nançay radio telescope (Table 1).

The OH radical in cometary atmospheres comes from the photodissociation of water, the major constituent of cometary ices. The direct observation of cometary water from the ground is difficult and one usually has to rely on secondary products such as OH to assess the outgassing of comets and its evolution. The OH radical can be observed through its A–X electronic system in the near UV, which can be done from the ground under good observing conditions (e.g., A'Hearn et al. 1995), or from space with dedicated instruments (e.g., Feldman 1999). The vibrational bands of OH can also be observed in the infrared (either from space or from the ground), but this has only been possible in a few cases. Radio observations of the 18-cm lines of OH are quite different from UV or infrared spectroscopic observations. Radio lines are fully resolved and their Doppler profiles allow us to investigate the kinematic properties of the cometary atmosphere. This is hardly possible at other wavelengths. The radio telescope beam samples a large part of the coma, so that minimal extrapolations to the whole coma are required (in contrast to typical visible or UV spectroscopic observations, which sample only a very small fraction of the coma). Radio observations at 18-cm wavelength do not have visibility constraints such as solar elongation and are almost insensitive to weather conditions. However, because of the particularities of the excitation mechanism of the OH radical, which depends upon the heliocentric radial velocity (see Sect. 3), the observation of the 18-cm OH lines is only possible part of the time.

The purpose of the present paper is to describe the set of cometary observations made at Nançay in the 1982–1999 period, that began with the implementation of an efficient autocorrelator spectrometer and ended with a major upgrading of the telescope.

The resulting spectra are now organized in a data base where they can be accessed interactively. Dedicated software[2] (XCOM) allows us to display and process the spectra, and to retrieve physical parameters such as the OH production rates using model parameters specified by the user.

Send offprint requests to: J. Crovisier,
e-mail: Jacques.Crovisier@obspm.fr

⋆ Appendix A, Table 2 and figures of the sum spectra are only available in electronic form at http://www.edpsciences.org The spectra and tables of the Appendix are only available in electronic form at the CDS via anonymous ftp to cdsarc.u-strasbg.fr (130.79.128.5) or via http://cdsweb.u-strasbg.fr/cgi-in/qcat?J/A+A/393/1053

⋆⋆ Deceased.

[1] The old-style designation is retained here for comets observed before 1995. Cross-references between old- and new-style designations are given in Table 1.

[2] Which is based upon the GILDAS software package (http://iram.fr/GS/gildas.html) developed at the Observatoire de Grenoble.

Table 1. The comets observed at Nançay up to 1999.

comet a)	b)	c)	perihelion [yymmdd]	q [AU]	range of observations [yymmdd]	r range d) [AU]	e)	f)	g)	h)
1973 XII	1973f	C/1973 E1 Kohoutek	731228.43	0.142	731129–740215			N	D	
1975 IX	1975h	C/1975 N1 Kobayashi-Berger-Milon	750905.33	0.426	750826–750904			L	D	
1976 VI	1975n	C/1975 V1 West	760225.22	0.197	760324–760512			L	D	
1977 XI		2P/Encke	770817.01	0.341	770808–770911			J	-	
1977 XIV	1977m	C/1977 R1 Kohler	771110.57	0.991	771021–771130			L	D	
1978 VII	1978c	C/1978 C1 Bradfield	780317.69	0.437	780304–780316			L	D	
1978 XXI	1978f	C/1978 H1 Meier	781111.41	1.137	780531–781029			N	D	
1979 X	1979l	C/1979 Y1 Bradfield	791221.60	0.545	800127–800203			L	M	
1980 XI		2P/Encke	801206.58	0.340	800919–801229			J	M	
1980 XII	1980q	C/1980 V1 Meier	801209.65	1.520	801116–810218			L	D	
1980 XV	1980t	C/1980 Y1 Bradfield	801229.54	0.260	810103–810303			L	M	
1981 XIX	1981j	64P/Swift-Gehrels	811127.27	1.361	811031–811111			J	–	
1982 I	1980b	C/1980 E1 Bowell	820312.29	3.364	821127–821219	4.17–4.29	15	N	–	1
1982 IV	1982a	26P/Grigg-Skjellerup	820515.00	0.989	820507–820625	0.99–1.15	15	J	–	2
1982 VI	1982g	C/1982 M1 Austin	820824.73	0.648	820626–820905	0.65–1.33	38	L	D	3
1982 VII	1982e	6P/d'Arrest	820914.31	1.291	820708–820823	1.32–1.51	34	J	M	4
1982 VIII	1982f	67P/Churyumov-Gerasimenko	821112.10	1.306	821009–821025	1.32–1.37	7	J	M	5
1984 IV	1983n	27P/Crommelin	840220.17	0.735	840121–840320	0.73–0.92	35	H	M	6
1984 XIII	1984i	C/1984 N1 Austin	840912.14	0.291	840727–840811	0.29–0.55	14	L	D	7
1985 XIII	1984e	21P/Giacobini-Zinner	850905.21	1.028	850331–851120	1.03–2.20	117	J	D	8
1985 XVII	1985l	C/1985 R1 Hartley-Good	851209.12	0.695	850924–860113	0.70–1.54	93	L	D	9
1985 XIX	1985m	C/1985 T1 Thiele	851219.21	1.317	851027–851216	1.32–1.53	35	L	D	10
1986 III	1982i	1P/1982 U1 Halley	860209.45	0.587	850126–860729	0.59–5.04	408	H	D	11
1987 II	1986n	C/1986 V1 Sorrells	870309.65	1.721	870101–870214	1.62–2.44	10	L	D	12
1987 III	1987c	C/1987 B1 Nishikawa-Takamizawa-Tago	870317.29	0.872	870303–870312	0.88–0.91	10	L	D	13
1987 VII	1986l	C/1986 P1 Wilson	870420.78	1.200	860825–870622	1.24–3.42	116	L	D	14
1987 XXIX	1987s	C/1987 P1 Bradfield	871107.26	0.869	871001–871128	0.89–1.09	34	L	D	15
1988 I	1987d_1	C/1987 W1 Ichimura	880110.10	0.200	880103–880109	0.78–0.99	7	L	M	16
1988 V	1988a	C/1988 A1 Liller	880331.11	0.841	880317–880324	0.85–0.88	6	L	D	17
1988 XV	1988j	C/1988 P1 Machholz	880917.57	0.165	880912–881019	0.26–0.97	18	L	–	18
1989 X	1989o	23P/1989 N1 Brorsen-Metcalf	890911.94	0.479	890804–891031	0.48–1.17	61	H	D	19
1989 XIX	1989r	C/1989 Q1 Okazaki-Levy-Rudenko	891111.92	0.642	891003–891202	0.64–1.03	49	N	D	20
1989 XXII	1989a_1	C/1989 W1 Aarseth-Brewington	891227.89	0.301	891208–891230	0.30–0.63	19	L	D	21
1990 V	1989c_1	C/1989 X1 Austin	900409.97	0.350	900215–900615	0.35–1.52	100	N	D	22
1990 XX	1990c	C/1990 K1 Levy	901024.63	0.939	900616–900930	1.03–2.26	77	L	D	23
1992 III	1991g_1	C/1991 Y1 Zanotta-Brewington	920131.99	0.644	920109–920129	0.72–0.92	17	N	D	24
1992 VII	1992b	C/1992 B1 Bradfield	920319.54	0.500	920301–920312	1.02–1.14	10	L	–	25
1992 VIII	1991h_1	C/1991 X2 Mueller	920321.20	0.199	920305–920318	0.22–0.56	12	N	–	26
1992 XIX	1991a_1	C/1991 T2 Shoemaker-Levy	920723.75	0.829	920610–920722	0.84–1.16	38	L	D	27
1992 XXVIII	1992t	109P/1992 S2 Swift-Tuttle	921212.33	0.958	921015–930112	0.96–1.36	54	H	D	28
1993 III	1992x	24P/Schaumasse	930303.96	1.202	930121–930220	1.21–1.32	30	J	D	29
1994 V		2P/Encke	940209.47	0.331	940111–940303	0.34–0.77	36	J	M	30
1994 IX	1993p	C/1993 Q1 Mueller	940326.31	0.967	940120–940320	0.97–1.45	40	N	D	31
1994 XI	1993v	C/1993 Y1 McNaught-Russell	940331.09	0.868	940301–940420	0.96–1.02	25	L	D	32
1994 XV	1992r	8P/Tuttle	940625.29	0.998	940604–940616	1.01–1.05	12	H	M	33
1994 XXVI	1994o	141P/1994 P1 Machholz 2	940918.63	0.753	940908–940914	0.76–0.77	7	J	M	34
1994 XXX	1994l	19P/Borrelly	941101.49	1.365	940905–950118	1.39–1.62	51	J	D	35
		15P/Finlay	950505.04	1.036	950405–950422	1.04–1.12	17	J	–	36
		C/1995 Q1 Bradfield	950831.42	0.436	950824–950926	0.47–0.83	18	L	D	37
		73P/Schwassmann-Wachmann 3	950922.75	0.933	950830–951101	0.94–1.10	36	J	D	38
		122P/1995 S1 de Vico	951006.02	0.659	951001–951020	0.67–0.72	10	H	D	39
		45P/Honda-Mrkos-Pajdušáková	951225.93	0.532	951125–960120	0.53–0.81	37	J	M	40
		C/1996 B2 Hyakutake	960501.40	0.230	960301–960518	0.23–1.51	49	L	D	41
		22P/Kopff	960702.19	1.580	960409–960523	1.63–1.78	40	J	D	42
		C/1996 Q1 Tabur	961103.53	0.840	961002–961027	0.85–1.03	17	L	D	43
		C/1995 O1 Hale-Bopp	970401.13	0.914	950804–970921	0.91–7.04	329	L	D	44
		46P/Wirtanen	970314.14	1.064	970204–970509	1.07–1.30	40	J	–	45
		81P/Wild 2	970506.64	1.583	970121–970323	1.64–1.88	37	J	M	46
		2P/Encke	970523.60	0.331	970513–970522	0.33–0.43	9	J	–	47
		C/1998 J1 SOHO	980508.62	0.153	980601–980608	0.79–0.96	8	L	D	48
		C/1998 P1 Williams	981017.84	1.147	980918–981004	1.17–1.24	12	L	M	49
		21P/Giacobini-Zinner	981121.32	1.034	981020–981115	1.04–1.13	22	J	D	50
		C/1998 U5 LINEAR	981221.89	1.236	981124–981210	1.25–1.30	15	L	M	51
		C/1999 H1 Lee	990711.17	0.708	990508–990814	0.71–1.39	66	L	D	52
		C/1999 N2 Lynn	990723.05	0.761	990716–990719	0.76–0.77	4	L	D	53

a) Old-style definitive designation; b) old-style provisional designation; c) new-style designation; d) lowest and highest heliocentric distances of the observations; e) number of observations in the data base; f) comet type; N: dynamically new, long-period comet; L: other long-period comet; H: Halley-type comet; J: Jupiter-family comet; g) –: no detection; M: marginal detection; D: clear detection; h) corresponding order number of the electronic tables and figures.

The scientific analysis of these data is beyond the scope of the present paper and is the subject of separate publications, present or future (Table 2):

- study of the excitation mechanisms of the OH radio lines (Biraud et al. 1974; Despois et al. 1981; Gérard 1990; Gérard et al. 1998; Colom et al. 1999);
- statistical analysis of the correlation between OH production rates and visual magnitudes (Despois et al. 1981; Bockelée-Morvan et al. 1981; Jorda 1995; Jorda et al. 1992, 1996);
- study of the long-term and short-term variability of the OH production rate in 1P/Halley (Gérard et al. 1987; Colom & Gérard 1988);
- analysis of the 18-cm line widths in relation with the expansion velocity of the atmosphere (Bockelée-Morvan & Gérard 1984; Bockelée-Morvan et al. 1990a);
- analysis of the 18-cm line profile in relation with anisotropic outgassing and non-gravitational forces (Bockelée-Morvan & Gérard 1984; Colom et al. 1990 and in preparation);
- study of the Zeeman effect and of its relation to the cometary magnetic field (Gérard 1985; Bockelée-Morvan et al. 1992; Gérard et al. 1993).

Section 2 describes the characteristics of the Nançay radio telescope and the observing procedures. Section 3 explains how OH production rates can be derived from the radio observations. Section 4 briefly recalls the 1973–1981 observations. Section 5 is a detailed description of the 1982–1999 observations while notes on individual comets are given in an Appendix. Section 6 discusses some statistical aspects of the data base. Section 7 concludes on the future of cometary observations at Nançay.

Most of the tables and figures of the present paper are only available in electronic form[3]. The Nançay spectra are public domain and may be requested from the CDS. The data base itself and its companion software XCOM are not transportable and cannot be remotely accessed. They could be used, however, in collaboration with the authors.

2. Observations

The Nançay radio telescope is a meridian instrument. It can observe sources at declination $\delta > -39°$ and can track them for about $\pm 1.1/\cos\delta$ hour. For observations at 18 cm wavelength, its RA × dec beam is $3.5' \times 19'$ at declinations lower than 30°. Its sensitivity for point sources is 0.9 K Jy^{-1} at $\delta \approx 0°$ and its variation with declination is given in Fig. 1 of Gérard et al. (1989). The system temperature was typically 45 K (at $\delta \approx 0°$) at the end of the observing period considered here.

[3] Via anonymous ftp to
cdsarc.u-strasbg.fr (130.79.128.5) or via
http://cdsweb.u-strasbg.fr/cgi-bin/qcat?J/A+A/393/1053
for the tables and the spectra (fits file) and to
http://www.edpsciences.org for the figures of the sum spectra.
Also independently available from
http://www.usr.obspm.fr/~crovisie/basecom/index.html

Since 1982, all cometary observations have been made using a 1024-channel autocorrelator split into 4 × 256–channel banks, allowing simultaneous observations of the OH 18-cm main lines at 1667 and 1665 MHz (except for occasional observations of the satellite lines at 1612 and 1721 MHz), and two polarizations (right- and left-circular polarizations, except for comets Bowell 1982 I and 6P/Churyumov-Gerasimenko 1982 VII which were observed in vertical and horizontal linear polarizations). In 1983, the Nançay radio telescope was closed for upgrading (installation of a new carriage house, of new computers and operating software). As a consequence, comets Sugano-Saigusa-Fujikawa 1983 V and IRAS-Araki-Alcock 1983 VII, which respectively passed at only 0.063 and 0.033 AU from the Earth, unfortunately could not be observed.

The autocorrelator is set to a 782 Hz channel separation, corresponding to 0.14 km s^{-1}. The effective resolution is 0.28 km s^{-1} after Hanning smoothing. A frequency-switching mode is used, with a frequency shift of 100 kHz. A $\sqrt{2}$ factor in the signal-to-noise ratio is gained after folding the spectra. The spectral coverage is about ±8 km s^{-1}, which is enough for observing cometary spectra with a good determination of the baselines since the cometary line widths are typically 2 km s^{-1}. The comets are tracked in position and velocity using an ephemeris computed from the latest available orbital elements (which, except otherwise stated, are those distributed by the Central Bureau for Astronomical Telegrams). The occasional errors which resulted from inaccurate ephemeris are discussed in the Appendix.

A check of the telescope performance and backend setup was done by frequently (usually every other day) observing the OH lines of the galactic source W12. The radial velocity scale was accurate within ±0.02 km s^{-1}.

Interferences of external origin were very rare during the whole period 1973–1999 because most of the cometary observations were made in the main lines at 1665 and 1667 MHz. The protected radio astronomy band has a primary status over the whole range 1660.0 MHz–1670.0 MHz while the radial velocity of the nucleus with respect to the telescope never shifts the rest frequency by more than 0.5 MHz. Strong interferences of internal origin, however, were recorded in early 1982 which ruined the 1665 MHz observations (e.g., comet Bowell 1982 I) when a new receiver front-end was installed with improper local oscillator setting.

3. OH production rates

The derivation of OH production rates from the observation of the OH 18-cm lines requires the knowledge of the excitation conditions of the OH radical and of its distribution within the coma; this has been debated for some time and some of the parameters necessary for the modelling of cometary OH are still poorly known. A brief discussion of the present situation and of the assumptions and parameters used in the present paper is now in order. The sets of parameters used in several previous studies and in the present work are summarized in Table 3.

The excitation through UV pumping and subsequent fluorescence leads to inversion (or anti-inversion) of the ground-state Λ-doublet of OH. Following pioneering works of

Biraud et al. (1974) and Mies (1974), this process was modelled by Despois et al. (1981) and Schleicher & A'Hearn (1988), leading to an evaluation of the OH inversion as a function of heliocentric radial velocity similar – within details – in the two studies. The most notable divergence between the two model inversion curves is the small difference in the heliocentric velocity at which the crossovers occur from an inverted to an anti-inverted ground state population. Observations indicate that the Despois et al. model is better at some crossing points, and the Schleicher et al. model is better at others (see Fig. 9 in Schleicher & A'Hearn 1988). We have adopted here the inversion curve of Despois et al. We recall that the derived OH production rates are roughly inversely proportional to the assumed inversion value. The reader may wish to avoid using production rates measured at times when the absolute value of the inversion is too small.

The OH Λ-doublet acts as a weak maser, amplifying (or attenuating) according to its inversion (or anti-inversion) the continuum background at the wavelengths of the 18-cm lines. Most of the time, the background temperature $T_{\rm bg}$ is close to 3 K, but it may be significantly higher when a comet crosses the galactic plane or an occasional discrete radio source. We have evaluated $T_{\rm bg}$ from the Stockert continuum survey at 1420 MHz (Reich & Reich 1986) performed with a 25′ beam, available as computer files. The 1420 MHz intensities are converted to 1667 MHz assuming a 2.7 K cosmic contribution and a galactic contribution with a mean spectral index of −2.6. Unfortunately, similar data south of −19° declination are not yet available as computer files; the default value $T_{\rm bg} = 3.0$ K is then assumed.

The inversion of the OH Λ-doublet may be quenched by collisions with ions and electrons. Neglecting this effect leads to an underestimation of the OH production rate, which explains the large discrepancies between UV and radio OH production rates obtained in the past. OH quenching was modelled by Despois et al. (1981), Schloerb (1988), Gérard (1990) and by Budzien (1992); see also recent studies by Gérard et al. (1998), Colom et al. (1999) and Schloerb et al. (1999). We have adopted the model of Gérard (1990) for which the radius $r_{\rm q}$ of the quenching region scales as:

$$r_{\rm q} \propto r\, Q[\mathrm{OH}]^{\frac{1}{2}}. \qquad (1)$$

$r_{\rm q} = 65\,000$ km has been determined for $r = 1.38$ AU and $Q[\mathrm{OH}] = 9.4\times10^{28}$ s^{-1} from the observations of comet Halley. It should be noted, however, that the theory of OH quenching is still poorly constrained by the observations. $r_{\rm q}$ and Q[OH] were derived through an iterative process. In some cases (especially when the quenching zone is larger than the telescope beam), this process did not correctly converge.

The space distribution of the OH radical is described by a Haser-equivalent model (Combi & Delsemme 1980). The water and OH-radical lifetimes are set to 8.5×10^4 and 1.1×10^5 s, respectively (Table 3). We have not tried to include the effects of solar variability: they are discussed by Cochran & Schleicher (1993) and Budzien et al. (1994). The water expansion velocity $v_{\rm exp}$ is known to depend upon the heliocentric distance and the gas production rate. As shown by Bockelée-Morvan et al. (1990a), it can be derived from the OH line shapes when they are observed with a good signal-to-noise ratio. For determining the production rates or their upper limits in weak comets, we assumed this velocity to be $v_{\rm exp} = 0.8$ km s^{-1}. The ejection velocity of the OH radical following water photodissociation was assumed to be 0.95 km s^{-1} (Crovisier 1989; Bockelée-Morvan et al. 1990a).

Choosing the best parameters for deriving Q[OH] is a difficult task. The user of XCOM can specify her/his preferred parameters. In order to derive automatically a uniform set of results, we have chosen in the present work to analyse and present the data with two sets of parameters: those described above (Col. 4 of Table 3), and *1986A* (Col. 2 of Table 3), which were parameters used at the time of the *International Halley Watch*. The latter set is particularly useful when the iterative process to evaluate the quenching radius does not properly converge. Of course, the resulting Q[OH] may differ from those we published elsewhere from the same observations.

For comets with reasonably small Q[OH] (typically $<10^{+28}$ s^{-1}) not too close to the Earth or to the Sun (typically $\Delta, r > 1$ AU), the correction for quenching is not important. For such comets, $v_{\rm exp}$ is also close to 0.8 km s^{-1}. In this case, the three last models of Table 3 lead to similar production rates. For other comets, neglecting quenching could lead to significantly underestimated production rates.

The water expansion velocity, uniformly set to $v_{\rm exp} = 0.8$ km s^{-1} in the present analysis, also leads to underestimated production rates for those comets which have higher velocities. Retrieving $v_{\rm exp}$ from line shapes (last model of Table 3), following Bockelée-Morvan et al. 1990a) requires spectra with high signal-to-noise ratios and is not appropriate to the automatic analysis we are presenting here. In extreme cases (1P/Halley and C/1995 O1 (Hale-Bopp) close to perihelion), $v_{\rm exp}$ could be as high as 2 km s^{-1}. In such cases, Q[OH] could be underestimated by about a factor of two, or even more taking into account the non-linearity of the correction for quenching.

In extreme cases where the comet is highly productive like C/1995 O1 (Hale-Bopp) or came very close to the Earth like C/1996 B2 (Hyakutake), retrieving Q[OH] from observations aimed at the comet centre position, which are dominated by the quenched region, may be very difficult or even impossible. Help could come, however, from the analysis of observations made at offset positions. Such analyses are not presented here, and the reader is referred to our specific studies of comets Hyakutake and Hale-Bopp (Gérard et al. 1998; Colom et al. 1999).

How do our radio OH production rates compare with those obtained by other means? Systematic observations of the water (or OH) production rates have been achieved for an important number of comets: from ground-based observations of the *A–X* band of OH (A'Hearn et al. 1995); from space observations of the same band by *IUE* (for which no homogeneous analysis has yet been published); from Lyman α observations with *SOHO/SWAN* (Mäkinen et al. 2001a).

Table 4 lists the highest OH production rates determined for each comet in our data base (using parameters of Col. 4 of Table 3). For comparison, the Table reports Q[OH] derived from the ground-based spectrophotometric observations of A'Hearn et al. (1995), and $Q[\mathrm{H_2O}]$ from the Lyman α

Table 3. Haser model parameters used in former and present analyses to derive water production rates for OH observations.

	standard	1986A [a]	Haser-equivalent[b] with quenching	Haser-equivalent[b] with quenching and trapezium
parent velocity [km s^{-1}]	–	–	0.8	from line shapes[c]
parent lifetime [s]	–	–	8.5×10^4	8.5×10^4
parent scale length [km]	80 000	60 000	–	–
daughter velocity [km s^{-1}]	1.5	1.4	0.95	0.95
daughter lifetime [s]	4×10^5	10^5	1.1×10^5	1.1×10^5
quenching	none	none	[2]	[2]
used by	[1]	[3] [4] this work	[5] this work	[5] [6]

[a] The OH observers agreed upon this set of parameters at the time of the *International Halley Watch*. Note that Schloerb et al. (1987) give, for 1986A, vectorial model parameters which, when converted into Haser-equivalent parameters, are similar to those listed here.
[b] The parent and daughter *Haser-equivalent* scale lengths are computed from the lifetimes and velocities according to the formulas of Combi & Delsemme (1980).
[c] Derived from the fit of a trapezium to the line shape, according to Bockelée-Morvan et al. (1990a).
References: [1]: Despois et al. (1981); [2]: Gérard (1990); [3]: Gérard et al. (1988, 1989); [4]: Schloerb et al. (1987); [5]: Bockelée-Morvan et al. (1994); [6]: Bockelée-Morvan et al. (1990a).

observations of *SOHO/SWAN* (Mäkinen et al. 2001a), when such data has been published for a comparable heliocentric distance. The production rates from the ground-based visible observations of OH are systematically weaker, by a factor of 2 to 3, than those from Nançay. This can be attributed to the choice of the Haser-model parameters adopted by A'Hearn et al. (1995) (they assumed a parent scale length of 24 000 km, much shorter than our value). There is a more sound agreement with the production rates from the Lyman α data set. It is beyond the scope of the present paper to present a more detailed comparison of these various production rate determinations, which would involve a case-by-case study of the time evolution of each comet.

4. Comets observed between 1973 and 1981

Table 1 gives the list of all comets observed at Nançay up to 1999.

Observations made in 1973–1981 are not described here. There are only partly incorporated in the data base. Most of them were reported in Biraud et al. (1974), Despois (1978), Despois et al. (1981), Bockelée-Morvan et al. (1981), and Bockelée-Morvan (1982). Some representative spectra are also reproduced in Arpigny et al. (1999). Further information concerning these comets may be obtained on request.

5. Comets observed between 1982 and 1999

The rationale for cometary observations at Nançay evolved with time. In 1982, using for the first time a new receiver with a versatile backend, we tried to observe almost every "possible" object: five comets were observed, but only Austin 1982 VI yielded high quality spectra warranting meaningful scientific analyses. In the following years, we tried to optimize the scientific return of the observations by focusing our choice on bright comets, or on comets for which an observing campaign was set up. With some exceptions, the observations were scheduled only at the moments when the excitation of the OH radical was favourable.

The detailed log of all the observations made in 1982–1999 is given in tables available electronically. There is one entry per daily observation of a given comet. At the end of the set of observations of a given comet we also give the parameters of the spectra integrated over selected periods. Selections of the most representative spectra, for individual day observations or averages of several days as listed in the tables, are also available electronically.

As an example, we show here the log table and the figures for comet 22P/Kopff (Table 5 and Fig. 1).

The table columns are organized as follows:

- Date of the observation (`date`) (or range of dates for integrations);
- Geocentric distance (`delta`);
- Heliocentric distance (`r`);
- Heliocentric radial velocity (`rdot`);
- Theoretical inversion of the OH maser (`inv`) according to Despois et al. (1981);
- Theoretical inversion of the OH maser (`inv`) according to Schleicher & A'Hearn (1988);
- Background brightness temperature (`Tbg`) evaluated as explained in Sect. 3;
- The line area and its rms error (`area`), evaluated from −2.25 to 2.25 km s^{-1};
- The line maximum intensity and its rms error (`S`);
- The line central velocity and its rms error (`Vo`);
- The line width at half maximum and its rms error (`dVo`). These three last items result from a Gaussian fit to the spectrum and are only listed when the signal-to-noise ratio of the line is larger than 3;
- The OH production rate and its rms error (or its 3–σ upper limit) (`Q[OH]`), using the *Haser-equivalent* model with

Table 4. Maximum production rates determined for each comet in the Nançay data base, compared with production rates from ground-based visible OH and Lyman α.

comet			Nançay[d)]		other observations		
a)	b)	c)	max Q[OH] [10^{28} s^{-1}]	r [AU]	max Q[OH] [10^{28} s^{-1}]	r [AU]	
1982 I	1980b	C/1980 E1 Bowell	<8.0	4.93			
1982 IV	1982a	26P/Grigg-Skjellerup	<1.5	1.10	0.04	1.12	e)
1982 VI	1982g	C/1982 M1 Austin	9.4	0.76			
1982 VII	1982e	6P/d'Arrest	≈0.3	1.40	0.36	1.41	e)
1982 VIII	1982f	67P/Churyumov-Gerasimenko	≈0.9	1.35	0.35	1.41	e)
1984 IV	1983n	27P/Crommelin	≈1.1	0.76	1.0	0.71	e)
1984 XIII	1984i	C/1984 N1 Austin	25.4	0.51			
1985 XIII	1984e	21P/Giacobini-Zinner	6.0	1.04	3.2	1.12	e)
1985 XVII	1985l	C/1985 R1 Hartley-Good	2.5	0.76	2.0	0.89	e)
1985 XIX	1985m	C/1985 T1 Thiele	3.9	1.33	1.5	1.41	e)
1986 III	1982i	1P/1982 U1 Halley	108.6	0.71	35.	0.71	e)
1987 II	1986n	C/1986 V1 Sorrells	8.5	1.79	7.6	1.78	e)
1987 III	1987c	C/1987 B1 Nishikawa-Takamizawa-Tago	11.3	0.90	3.8	1.12	e)
1987 VII	1986l	C/1986 P1 Wilson	19.6	1.35			
1987 XXIX	1987s	C/1987 P1 Bradfield	9.5	0.93	3.9	1.12	e)
1988 I	1987d$_1$	C/1987 W1 Ichimura	12.9?	0.26			
1988 V	1988a	C/1988 A1 Liller	10.7	0.86	4.2	1.12	e)
1988 XV	1988j	C/1988 P1 Machholz	<0.8	0.81			
1989 X	1989o	23P/1989 N1 Brorsen-Metcalf	23.5	0.53			
1989 XIX	1989r	C/1989 Q1 Okazaki-Levy-Rudenko	7.6	0.65			
1989 XXII	1989a$_1$	C/1989 W1 Aarseth-Brewington	20.7	0.58			
1990 V	1989c$_1$	C/1989 X1 Austin	44.4	0.38			
1990 XX	1990c	C/1990 K1 Levy	20.6	1.06			
1992 III	1991g$_1$	C/1991 Y1 Zanotta-Brewington	1.3	0.75			
1992 VII	1992b	C/1992 B1 Bradfield	<1.3	0.58			
1992 VIII	1991h$_1$	C/1991 X2 Mueller	<2.4	0.43			
1992 XIX	1991a$_1$	C/1991 T2 Shoemaker-Levy	2.9	1.11	1.5	0.89	e)
1992 XXVIII	1992t	109P/1992 S2 Swift-Tuttle	54.2	0.97	25.	0.89	e)
1993 III	1992x	24P/Schaumasse	1.0	1.28			
1994 V		2P/Encke	≈1.3	0.50			
1994 IX	1993p	C/1993 Q1 Mueller	4.9	0.99			
1994 XI	1993v	C/1993 Y1 McNaught-Russell	4.4	0.94			
1994 XV	1992r	8P/Tuttle	≈3.2	1.03			
1994 XXVI	1994o	141P/1994 P1 Machholz 2	≈1.3	0.76			
1994 XXX	1994l	19P/Borrelly	2.8	1.43			
		15P/Finlay (1995)	<2.5	1.08			
		C/1995 Q1 Bradfield	17.5 ?	0.46			
		73P/Schwassmann-Wachmann 3 (1995)	22.2	0.95			
		122P/1995 S1 de Vico (1995)	61.0	0.68			
		45P/Honda-Mrkos-Pajdušáková (1996)	≈1.5	0.55	0.5	0.85	f)
		C/1996 B2 Hyakutake	20.3	0.70	56.	0.54	f)
		22P/Kopff (1996)	2.9	1.68			
		C/1996 Q1 Tabur	4.2	0.99	4.2	0.92	f)
		C/1995 O1 Hale-Bopp	463.3	0.92	1020.	0.91	f)
		46P/Wirtanen (1997)	<1.5	1.12	1.5	1.08	f)
		81P/Wild 2 (1997)	≈0.8	1.74			
		2P/Encke (1997)	<4.6	0.39	0.9	0.81	f)
		C/1998 J1 SOHO	30.3	0.87	71.	0.32	f)
		C/1998 P1 Williams	≈8.1	1.19			
		21P/Giacobini-Zinner (1998)	5.1	1.05			
		C/1998 U5 LINEAR	≈1.4	1.26			
		C/1999 H1 Lee	13.9	0.85			
		C/1999 N2 Lynn	6.4	0.77			

a) Old-style definitive designation; b) old-style provisional designation; c) new-style designation (with year of perihelion for recent short-period comets); d) using parameters of Col. 4 in Table 3, see text; e) from visible observations of OH (A'Hearn et al. 1995); f) from Lyman α observations (Mäkinen et al. 2001a).

Table 5. Detailed log of the observations of comet 22P/Kopff and results for integrations over selected periods of time (from Tables A.42a and A.42b). A comprehensive data set for all comets is available electronically.

NANCAY 22P/Kopff

date	delta AU	r AU	rdot km/s	inv	inv	Tbg K	area mJy km/s		S mJy		Vo km/s	dVo km/s	Q[OH] E28s-1	Q[OH] E28s-1	Fig.
960409-960412	1.13	1.78	-7.6	-0.31	-0.37	4.9	-85	12	-34	5	-0.03 0.18	2.34 0.45	2.5 0.4	2.6 0.4	A42.a
960419-960425	1.01	1.73	-6.8	-0.30	-0.36	10.2	-180	10	-94	5	-0.12 0.05	1.87 0.13	2.3 0.1	2.5 0.1	A42.a
960427-960430	0.94	1.71	-6.4	-0.29	-0.34	11.4	-296	11	-122	5	-0.22 0.05	2.16 0.11	2.9 0.1	3.2 0.1	A42.a
960501-960508	0.88	1.68	-5.9	-0.27	-0.33	5.3	-114	8	-60	3	-0.14 0.06	1.95 0.15	2.9 0.2	3.1 0.2	A42.a
960510-960515	0.81	1.66	-5.2	-0.25	-0.30	4.5	-92	11	-44	5	-0.22 0.11	1.94 0.28	2.7 0.3	2.7 0.3	A42.a
960516-960523	0.76	1.64	-4.6	-0.23	-0.27	4.3	-62	9	-38	4	-0.30 0.09	1.52 0.23	2.0 0.3	2.0 0.3	A42.a

NANCAY 22P/Kopff

date	delta AU	r AU	rdot km/s	inv	inv	Tbg K	area mJy km/s		S mJy		Vo km/s	dVo km/s	Q[OH] E28s-1	Q[OH] E28s-1	Fig.
96/04/ 9.19	1.15	1.78	-7.7	-0.31	-0.37	4.9	-90	25	-48	15	0.75 0.25	0.85 0.59	1.3 0.4	1.3 0.4	A42.b
96/04/10.19	1.14	1.78	-7.6	-0.31	-0.37	4.9	-67	24					<2.1	<2.2	A42.b
96/04/11.18	1.13	1.78	-7.5	-0.31	-0.37	4.8	-87	24	-42	12	-0.20 0.29	2.06 0.72	2.7 0.7	2.8 0.8	A42.b
96/04/12.18	1.11	1.77	-7.5	-0.31	-0.37	4.8	-96	26	-48	12	-0.14 0.31	1.95 0.77	2.8 0.8	3.0 0.8	A42.b
96/04/13.18	1.10	1.77	-7.4	-0.31	-0.37	5.0	6	30					<2.4	<2.6	A42.b
96/04/14.18	1.09	1.76	-7.4	-0.31	-0.37	5.2	-12	24					<2.0	<2.0	A42.b
96/04/19.17	1.04	1.74	-7.0	-0.31	-0.37	7.1	-150	26	-71	11	-0.87 0.19	2.55 0.48	3.3 0.6	3.7 0.7	A42.c
96/04/20.17	1.03	1.74	-7.0	-0.31	-0.36	7.7	-137	27	-66	11	0.02 0.17	1.98 0.41	2.3 0.5	2.5 0.5	A42.c
96/04/21.17	1.01	1.73	-6.9	-0.30	-0.36	8.4	-139	22	-60	11	-0.05 0.19	2.23 0.48	2.1 0.3	2.3 0.4	A42.c
96/04/22.17	1.00	1.73	-6.8	-0.30	-0.36	9.6	-115	24	-106	14	0.02 0.09	1.29 0.23	2.0 0.4	2.1 0.4	A42.c
96/04/23.17	0.99	1.73	-6.8	-0.30	-0.36	11.6	-307	22	-146	12	-0.14 0.08	1.98 0.20	3.1 0.2	3.5 0.3	A42.c
96/04/24.17	0.98	1.72	-6.7	-0.30	-0.35	12.8	-132	41	-121	20	0.60 0.18	2.01 0.44	2.7 0.8	2.7 0.8	A42.c
96/04/25.16	0.97	1.72	-6.6	-0.30	-0.35	17.5	-292	32	-147	17	-0.36 0.11	1.87 0.27	2.1 0.2	2.2 0.2	A42.d
96/04/26.16	0.96	1.71	-6.5	-0.29	-0.35	26.0	-4138	353	-1919	91	-2.44 0.12	7.11 0.39	0.0 0.0	0.0 0.0	A42.d
96/04/27.16	0.95	1.71	-6.5	-0.29	-0.35	21.1	-538	27	-214	12	-0.11 0.06	2.23 0.16	2.8 0.1	3.2 0.2	A42.d
96/04/28.16	0.94	1.71	-6.4	-0.29	-0.34	10.4	-234	23	-94	10	-0.16 0.12	2.32 0.29	2.6 0.3	2.9 0.3	A42.d
96/04/29.16	0.93	1.70	-6.3	-0.29	-0.34	6.5	-214	26	-81	11	-0.51 0.15	2.23 0.37	3.4 0.4	3.9 0.5	A42.d
96/04/30.16	0.92	1.70	-6.2	-0.29	-0.34	6.4	-176	23	-98	12	-0.31 0.11	1.78 0.27	3.4 0.4	3.8 0.5	A42.d
96/05/ 1.15	0.91	1.70	-6.2	-0.28	-0.34	6.1	-179	26	-75	12	-0.38 0.15	1.94 0.38	3.0 0.4	3.3 0.5	A42.e
96/05/ 2.15	0.90	1.69	-6.1	-0.28	-0.33	5.9	-132	25	-71	13	-0.07 0.18	1.85 0.44	2.9 0.6	3.1 0.6	A42.e
96/05/ 3.15	0.89	1.69	-6.0	-0.28	-0.33	5.6	73	35					<2.3	<2.5	A42.e
96/05/ 4.15	0.89	1.69	-5.9	-0.28	-0.33	5.3	-144	22	-82	11	0.07 0.12	1.76 0.29	3.4 0.5	3.7 0.6	A42.e
96/05/ 5.15	0.88	1.68	-5.8	-0.27	-0.32	5.1	-156	25	-72	11	0.14 0.20	2.35 0.49	4.2 0.7	4.6 0.7	A42.e
96/05/ 6.15	0.87	1.68	-5.8	-0.27	-0.32	4.9	-162	27	-61	10	-0.16 0.20	2.60 0.50	4.2 0.7	4.5 0.8	A42.e
96/05/ 7.14	0.86	1.68	-5.7	-0.27	-0.32	4.8	-83	24	-59	11	-0.53 0.18	1.27 0.45	2.1 0.6	2.2 0.6	A42.f
96/05/ 8.14	0.85	1.67	-5.6	-0.27	-0.31	4.6	-109	25	-60	14	0.07 0.20	1.89 0.49	3.3 0.7	3.4 0.8	A42.f
96/05/10.14	0.83	1.67	-5.4	-0.26	-0.31	4.5	-97	30	-67	15	-0.08 0.17	1.27 0.42	2.6 0.8	2.6 0.8	A42.f
96/05/11.14	0.82	1.66	-5.3	-0.26	-0.30	4.5	-173	31	-62	14	-0.09 0.23	2.22 0.56	4.3 0.8	4.3 0.8	A42.f
96/05/12.14	0.82	1.66	-5.3	-0.25	-0.30	4.5	-50	22					<2.0	<2.0	A42.f
96/05/13.13	0.81	1.66	-5.2	-0.25	-0.30	4.4	-97	22	-37	10	-0.42 0.28	2.20 0.70	2.6 0.6	2.6 0.6	A42.f
96/05/14.13	0.80	1.65	-5.1	-0.25	-0.29	4.4	-84	22	-31	9	0.10 0.39	2.97 0.99	3.0 0.8	3.0 0.8	A42.g
96/05/15.13	0.79	1.65	-5.0	-0.24	-0.29	4.4	-74	43					<4.0	<3.9	A42.g
96/05/16.13	0.78	1.65	-4.9	-0.24	-0.28	4.4	-87	29	-54	19	0.09 0.25	0.99 0.61	1.8 0.6	1.7 0.6	A42.g
96/05/17.13	0.78	1.65	-4.8	-0.24	-0.28	4.3	-82	22	-42	10	-0.25 0.23	2.32 0.57	3.4 0.9	3.2 0.9	A42.g
96/05/18.12	0.77	1.64	-4.7	-0.23	-0.27	4.3	-126	38	-37	15	-0.31 0.51	2.75 1.28	3.6 1.1	3.4 1.0	A42.g
96/05/19.12	0.76	1.64	-4.6	-0.23	-0.27	4.3	-56	24					<2.4	<2.3	A42.g
96/05/20.12	0.75	1.64	-4.5	-0.23	-0.26	4.3	-81	22	-51	15	-0.55 0.19	0.89 0.46	1.7 0.5	1.5 0.4	A42.h
96/05/21.12	0.75	1.64	-4.4	-0.22	-0.26	4.3	0	32					<2.9	<3.1	A42.h
96/05/22.12	0.74	1.63	-4.3	-0.22	-0.25	4.2	-20	26					<2.3	<2.6	A42.h
96/05/23.11	0.73	1.63	-4.3	-0.21	-0.25	4.2	-47	20					<2.0	<2.0	A42.h

quenching (Table 3, Col. 3) and the Despois et al. maser inversion. Null values are listed when the iterative algorithm to evaluate the quenching does not converge;

– The OH production rate and its rms error (or its 3–σ upper limit) (`Q[OH]`), using the *1986A* model (Table 3, Col. 2);

– The reference of the figure (`Fig.`) where the spectrum is shown.

When observations at offset positions were made, they are listed in a separate table in which the offsets (`offRA` and `offDec`) are listed instead of production rates.

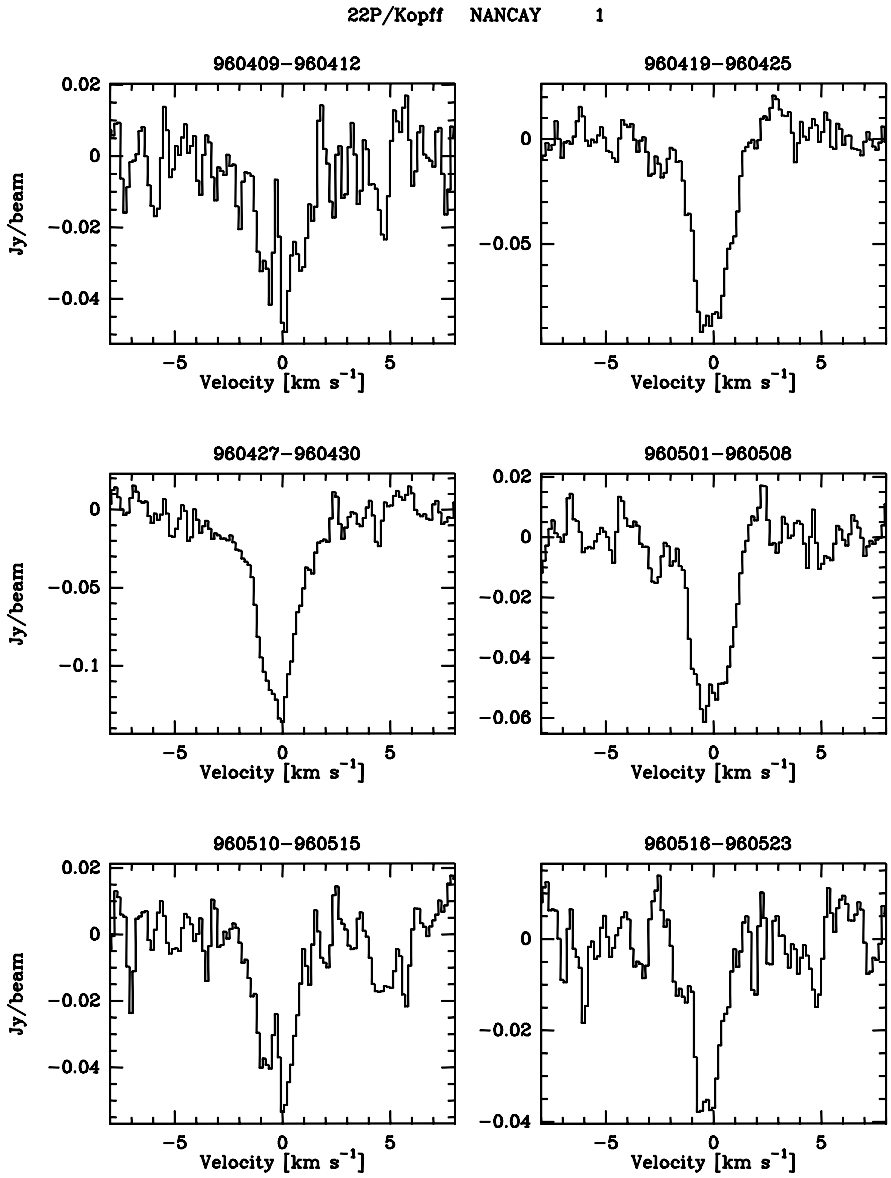

Fig. 1. Selection of representative spectra: comet 22P/Kopff (from Fig. A.42a). The spectra are integrated over selected periods of time, as given in Table 5. A comprehensive data set for all comets is available electronically.

Table 6. Comets observed at Nançay from 1973 to 1999: statistics of detections.

comet type	clear detection	marginal detection	not detected	total
long-period comets				
dynamically new	6	0	2	8
others	25	4	2	31
short-period comets				
Halley-type	4	2	0	6
Jupiter-family	5	6	4	15
total	40	12	8	60

Unless otherwise specified, the spectra shown in the figures are sums of the left- and right-handed circular polarizations and of the 1667 and 1665 MHz components, normalized to the 1667 MHz intensity (assuming the LTE ratio 1665:1667 = 5:9).

The individual observations of each comet are discussed separately in Appendix A.

6. Statistics

From 1973 to 1999, we observed 60 different comets at Nançay (not counting multiple returns). 40 were clearly detected, and 12 marginally detected. Table 6 lists the distribution of these detections among different families of comets, as listed in Table 1. Among long-period comets ($P > 200$ years), we have distinguished dynamically new comets (with semi major axis $a > 20\,000$ years) from others (with smaller a, or for which a could not be precisely determined). Among short-period comets, we have separated Jupiter-family ($P < 20$ years,

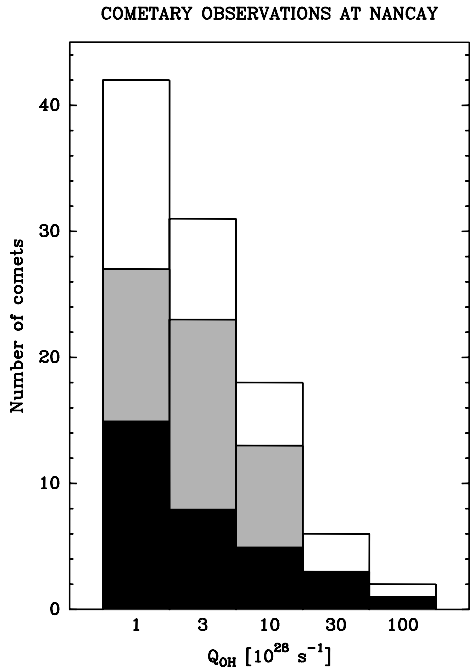

Fig. 2. Histograms of the number of comets with Q[OH] observed larger than a given value. Three histograms are superimposed: short-period comets (black), long-period comets (grey) and full sample (white).

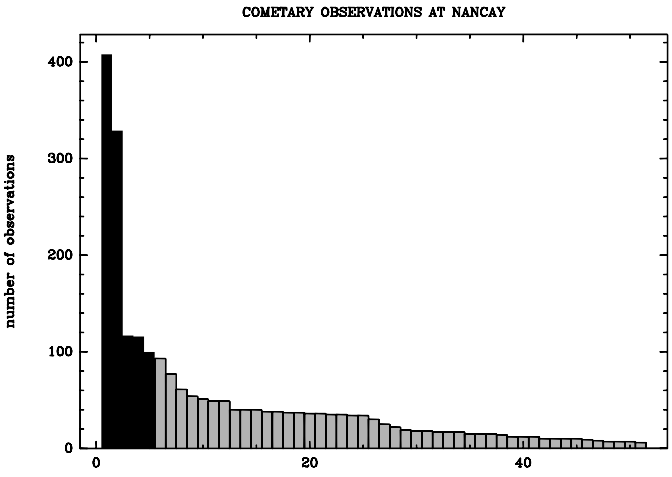

Fig. 3. Histogram of the number of observations per comet. The abscissa is a ranking number in order of number of observations. In Figs. 3 to 7, the black part of the histograms refer to the five most-observed comets.

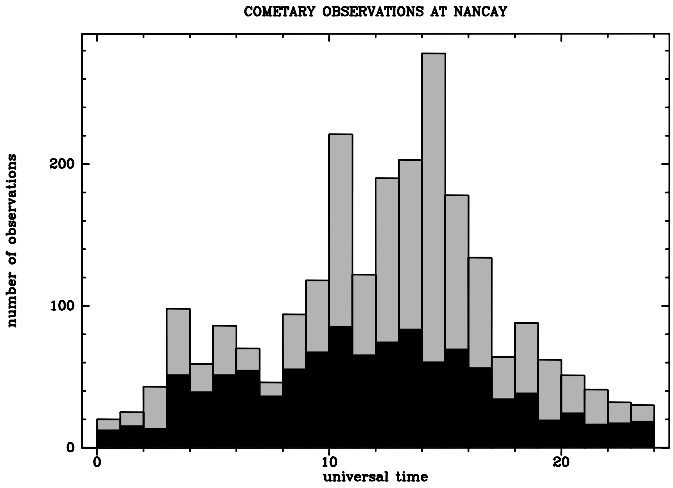

Fig. 4. Distribution of the observations as a function of universal time.

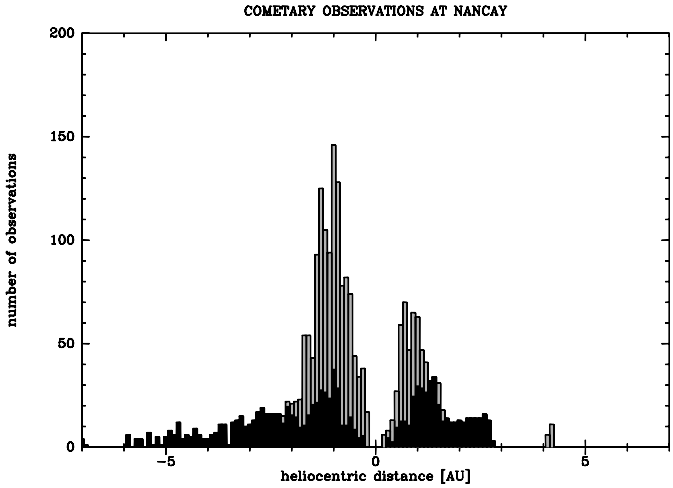

Fig. 5. Distribution of the observations as a function of heliocentric distance (negative: pre-perihelion; positive: post-perihelion).

small inclination) and Halley-type ($20 < P < 200$ years, random inclination) comets.

The upper limit that can be achieved on Q[OH] depends on r, Δ and the inversion i of the OH maser. For observations spread over one week (7×1 hour integration), the 3–σ upper limit on the line area is $\approx$0.030 K km s^{-1}. This corresponds to an upper limit Q[OH] $< 1.3 \times 10^{28}$ s^{-1} for a comet at $r = \Delta = 1$ AU with $i = 0.3$. Few comets, with better observing conditions, were detected with Q[OH] $< 10^{28}$ s^{-1}.

Figure 2 shows the distribution of comets with Q[OH] larger than a given value (Q being the strongest OH production rate obtained during the scheduled observations of the comet, as listed in Table 4). There is an average of one comet per year observed with Q[OH] $> 10^{29}$ s^{-1}. We believe that we have not missed any comet at this production rate level, in the sky domain accessible to Nançay. Some comets, however, may have reached higher Q[OH] than those we observed, because radio observations of OH close to perihelion or at small heliocentric distances are more difficult (unfavourable OH maser inversion, higher quenching, smaller OH lifetime). Comets with small ($<3 \times 10^{28}$ s^{-1}) Q[OH] are grossly under represented, because of the detection limit discussed above, and because observations of such weak comets were less frequently scheduled.

Figures 3–7 show some other aspects of the distribution of the Nançay observations. No discrimination has been made between observations with or without detection. Figure 3 is the histogram of the number of daily observations per comet. Five comets with 100 or more observations were the object of a peculiarly long campaign of observation and represent 45% of all observations. They are 1P/Halley, C/1995 O1 (Hale-Bopp), 21P/Giacobini-Zinner (1985 return), C/1986 P1 (Wilson) and

C/1989 X1 (Austin), in order of decreasing number of observations. In Figs. 3, 4, 5 and 7, these well-studied comets are shown as black histograms, superimposed over grey histograms for the full sample.

Figure 4 is the histogram of the observations as a function of UT time. At Nançay, civil time is UT+8^{m}. The distribution shows that day-time observations are more numerous by a significant factor (1718 observations between 6.0 and 18.0 UT, to be compared to only 635 in the other UT hours). This is because observations were preferentially made when the comets are the most productive, which is when they are close to the Sun and therefore at small solar elongation. Why the distribution actually peaks in the afternoon is not understood. No significant trend is found in the distribution as a function of sideral time.

Figure 5 is the distribution of the heliocentric distances at which observations were made. More observations were made pre-perihelion rather than post-perihelion; the explanation is discussed with Fig. 7. Observations at more than ≈2 AU were only attempted in the brightest comets, among the five well-studied objects (except for comet Bowell (1982 I), which was observed – and undetected – at ≈4 AU post-perihelion).

Figure 6 shows together the distributions of heliocentric and geocentric distances of the observations (irrespective of the pre- or post-perihelion situation). We see that observations were generally made at smaller geocentric than heliocentric distances. This is still a consequence of our aim to make observations in the best observing conditions.

Figure 7 shows the distribution of the heliocentric radial velocities of the observations. This obviously uneven distribution can be easily understood: the excitation of the cometary OH maser strongly depends upon the heliocentric radial velocity and the signal is expected, in first approximation, to be proportional to the maser inversion. As a consequence, the observations were preferentially planned at the moments of strong inversions. The theoretical maser inversion is also plotted in the figure to show this correlation. Only for bright comets were observations made at the moment of weak inversion, to investigate other possible excitation mechanisms. On the average, the inversion is weaker post-perihelion (positive heliocentric velocities) compared to pre-perihelion. Accordingly, post-perihelion observations are less numerous.

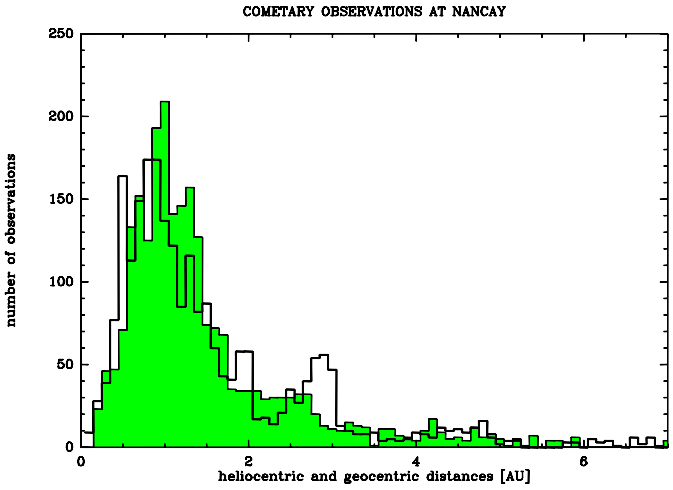

Fig. 6. Distribution of the observations as a function of heliocentric (in grey) and geocentric (plain thick line) distances.

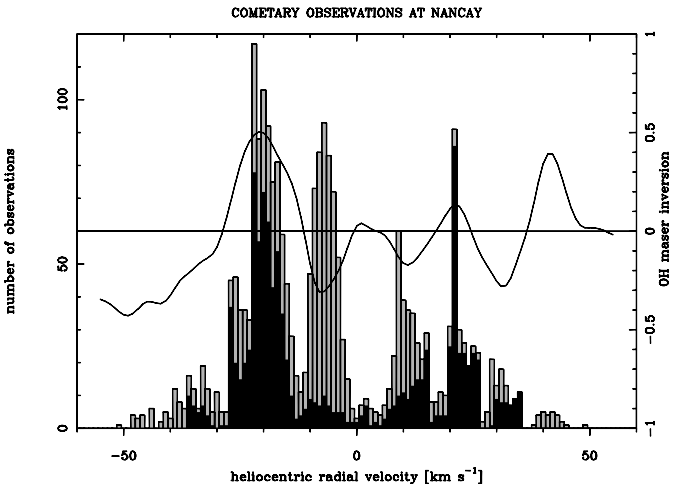

Fig. 7. Distribution of the observations as a function of heliocentric radial velocity. The OH maser inversion (from Despois et al. 1981) is also plotted.

7. Conclusion and prospects

We have attempted to present a most complete and comprehensive view of all the valuable OH cometary data taken at Nançay since 1973. The scientific exploitation of the data base is quite incomplete and it is hoped that the present paper will stir up new ideas and collaborations.

Clearly, some studies are lagging because the physics of OH cometary masers is not fully understood (e.g., the quenching mechanism and the non-thermal excitation of the OH transitions). This is also the case of the relation between the anisotropic outgassing and the non-gravitational forces, the average cometary magnetic field and its relation with the solar magnetic field structure. It is also true that the interest of cometary researchers has strongly shifted to millimetre wavelengths where many fundamental microwave lines have been discovered.

The Nançay radio telescope has undergone a major upgrade which started in 1995 and ended in 2000 (van Driel et al. 1996). The old Hoghorn feeds were replaced by a double Gregorian wide-band system with corrugated horns and sensitivity improved by a factor of 2.2. Furthermore, the horns can be rotated by ±90° and provide full polarization capability. Thus, if the OH cometary maser is linearly polarized with an expected minimum along the comet–Sun direction (Mies 1976), the position angle of the orthogonal polarizations can be set in this direction[4]. A new autocorrelator has also been constructed which provides for cometary observations 8 banks of 1024 channels in 195 kHz (190 Hz channel separation, corresponding to 0.035 km s^{-1}, or 0.07 km s^{-1} after Hanning smoothing). As in

[4] However, the Larmor frequency of OH due to the weak magnetic field in the coma is much higher than the UV excitation rate of this radical. The polarization geometry could thus be dominated by the magnetic field rather than the Sun direction.

the past, a frequency-switching mode is used and subsequent folding results in a gain of a factor of 1.4. It is now possible to observe simultaneously the four OH transitions at 1665 and 1667 MHz (main lines) and 1612 and 1721 MHz (satellite lines) in both left- and right-hand circular polarizations, to detect possible Zeeman shifts and departures from the LTE line intensity ratios.

The new system has been successfully used already since July 2000 to detect four comets in 2000, namely C/1999 S4 (LINEAR) in early July 2000, before its disintegration (Bockelée-Morvan et al. 2001), C/1999 T1 (McNaught-Hartley) in November–December 2000, 73/P Schwassmann-Wachmann 3, and C/2000 W1 (Utsunomiya-Jones) in December 2000. These new observations will described in future publications.

With an increased sensitivity by a factor 2.2, one can either start observing "usual" comets at larger heliocentric distances or detect intrinsically fainter objects, or perform a more continuous monitoring of these objects. Alternately, one may wish to study the long- and short-term variations of the OH production rate associated with the outbursts, break-up of the cometary nuclei and correlate them with the production rates variations of other species and/or with the visual magnitude. Whatever the future strategy, the new system should allow to handle several cometary observations daily much more easily than in the past.

Acknowledgements. This paper is dedicated to the memory of Odile Franquelin and Gabriel Bourgois, who died during the course of this work.

Thanks are due to other observers in the early days of this programme (F. Biraud, I. Kazès, D. Despois and N. Hallet) for their help and to other members or visitors of the *groupe comètes* at Meudon (L. Jorda, N. Biver and H. Rauer) for their support.

The observations at Nançay would not have been possible without the help and support of the operators and of the technical staff of the radio telescope. These observations blindly rely on cometary ephemeris; we are very grateful to those who provided timely astrometric positions and orbital elements (B. Marsden and D. Green at the Central Bureau for Astronomical Telegrams, D. Yeomans at the Jet Propulsion Laboratory, and P. Rocher at the Bureau des longitudes).

The Nançay Radio Observatory is the Unité scientifique de Nançay of the Observatoire de Paris, associated as Unité de service et de recherche (USR) No. B704 to the French Centre national de la recherche scientifique (CNRS). The Nançay Observatory also gratefully acknowledges the financial support of the Conseil régional of the Région Centre in France.

References

A'Hearn, M. F., Millis, R. L., Schleicher, D. G., Osip, D. J., & Birch, P. V. 1995, Icarus, 118, 223

A'Hearn, M. F., Schleicher, D. G., Millis, R. L., Feldman, P. D., & Thompson, D. T. 1984, AJ, 89, 579

Arpigny, C., Dossin, F., Woszczyk, N., et al. 1999, Atlas of Cometary Spectra (Kluwer), in press

Bertaux, J.-L., Costa, J., Mäkinen, T., et al. 1999, Planet. Space Sci., 47, 725

Biraud, F., Bourgois, G., Crovisier, J., et al. 1974, A&A, 34, 163

Biver, N., Bockelée-Morvan, D., Colom, P., et al. 1997, Science, 275, 1915

Biver, N., Bockelée-Morvan, D., Colom, P., et al. 1999a, Earth Moon Planets, 78, 11

Biver, N., Bockelée-Morvan, D., Colom, P., et al. 1999b, IAU Circ., 7203

Biver, N., Bockelée-Morvan, D., Crovisier, J., et al. 2000, AJ, 120, 1554

Biver, N., Rauer, H., Despois, D., et al. 1996, Nature, 380, 137

Black, J. H., Chaisson, E. J., Ball, J. A., Penfield, H., & Lilley, A. E. 1974, ApJ, 191, L45

Bockelée-Morvan, D. 1982, Production, Cinématique et Asymétries de la Coma OH dans les Comètes C/Meier 1978 (XXI), C/Bradfield (1979 X), C/Meier (1980q), C/Bradfield (1980t) et Encke, Thèse de 3e cycle, Université Paris VI

Bockelée-Morvan, D., Biver, N., Colom, P., et al. 1995, Bull. Amer. Astron. Soc., 27, 1144

Bockelée-Morvan, D., Biver, N., Moreno, R., et al. 2001, Science, 292, 1339

Bockelée-Morvan, D., Bourgois, G., Colom, P., et al. 1994, Planet. Space Sci., 42, 193

Bockelée-Morvan, D., Bourgois, G., Crovisier, J., & Gérard, E., 1989, IAU Circ., 4882

Bockelée-Morvan, D., Colom, P., Crovisier, J., Gérard, E., & Bourgois, G. 1992, in Asteroids, Comets, Meteors 1991, ed. A. W. Harris, & E. Bowell, 73

Bockelée-Morvan, D., Crovisier, J., & Gérard, E. 1990a, A&A, 238, 382

Bockelée-Morvan, D., Crovisier, J., Gérard, E., & Bourgois, G. 1990b, in Workshop on Observations of Recent Comets, ed. W. F. Huebner, J. Rahe, P. A. Wehinger, & I. Konno, 75

Bockelée-Morvan, D., Crovisier, J., Gérard, E., et al. 1985, AJ, 90, 2586

Bockelée-Morvan, D., Crovisier, J., Gérard, E., & Kazès, I. 1981, Icarus, 47, 464

Bockelée-Morvan, D., & Gérard, E. 1984, A&A, 131, 111

Bockelée-Morvan, D., Padman, R., Davies, J. K., & Crovisier, J. 1994, Planet. Space Sci., 42, 655

Budzien, S. A. 1992, Physical and chemical processes of the inner coma observed in mid-ultraviolet cometary spectra, Ph.D. dissertation, Johns Hopkins University

Budzien, S. A., Festou, M. C., & Feldman, P. D. 1994, Icarus, 107, 164

Cochran, A. L., & Schleicher, D. G. 1993, Icarus, 105, 235

Colom, P., Bockelée-Morvan, D., Bourgois, G., et al. 1992, IAU Circ., 5643

Colom, P., & Gérard E. 1988, A&A, 204, 327

Colom, P., Gérard, E., & Crovisier, J. 1990, in Asteroids Comets Meteors III, ed. C.-I. Lagerkvist, H. Rickman, B. A. Lindblad, & M. Lindgren, 293

Colom, P., Gérard, E., Crovisier, J., et al. 1999, Earth Moon Planets, 78, 37

Combi, M. R., & Delsemme, A. H. 1980, ApJ, 237, 633

Crovisier, J. 1989, A&A, 213, 459

Crovisier, J. 1992, in Asteroids, Comets Meteors 1991, ed. A. W. Harris, & E. Bowell, 137

Crovisier, J., Bockelée-Morvan, D., Colom, P., Gérard, E., & Biver, N. 1998, IAU Circ., 6934

Crovisier, J., Biver, N., Bockelée-Morvan, D., et al. 1995, IAU Circ., 6227

Crovisier, J., Biver, N., Bockelée-Morvan, D., et al. 2001, ESA SP-1165, in press

Crovisier, J., Bockelée-Morvan, D., Bourgois, G., & Gérard, E. 1992, A&A, 253, 286

Crovisier, J., Bockelée-Morvan, D., Gérard, E., et al. 1996a, A&A, 310, L17
Crovisier, J., Despois, D., Bockelée-Morvan, D., et al. 1990, A&A, 234, 535
Crovisier, J., Despois, D., Bockelée-Morvan, D., & Gérard, E. 1987, IAU Circ., 4411
Crovisier, J., Gérard, E., Colom, P., et al. 1996b, IAU Circ., 6394
Crovisier, J., & Schloerb, F. P. 1991, in Comets in the Post-Halley Era, ed. R. L. Newburn, M. Neugebauer, & J. Rahe (Kluwer, Dordrecht), 149
Deich, W. T. S., Cordes, J. M., & Terzian, Y. 1985, AJ, 90, 373
de Pater, I., Palmer, P., & Snyder L. E. 1991, in Comets in the Post-Halley Era, ed. R. L. Newburn, M. Neugebauer, & J. Rahe (Kluwer, Dordrecht), 175
Despois, D. 1978, Étude Radio Astronomique du Radical OH dans les Comètes, Thèse de 3e cycle, Université Paris VI
Despois, D. 1999, Earth Moon Planets, 79, 103
Despois, D., Biver, N., Bockelée-Morvan, D., et al. 1996, Planet. Space Sci., 44, 529
Despois, D., Gérard, E., Crovisier, J., & Kazès, I. 1981, A&A, 99, 320
Farnham, T., & Schleicher, D. 1998, A&A, 335, L50
Feldman, P. D. 1999, Earth Moon Planets, 79, 145
Festou, M. C., Feldman, P. D., & A'Hearn, M. F. 1992, in Asteroids, Comets Meteors 1991, ed. A. W. Harris, & E. Bowell, 177
Fink, U., Hicks, M. P., & Fevig, R. A. 1999, Icarus, 141, 331
Gérard, E. 1985, A&A, 146, 1
Gérard, E. 1987, in Workshop on Cometary Radio Astronomy, NRAO Workshop No. 17, 91
Gérard, E. 1990, A&A, 230, 489
Gérard, E., Bockelée-Morvan, D., Bourgois, G., Colom, P., & Crovisier, J. 1986, IAU Circ., 4271
Gérard, E., Bockelée-Morvan, D., Bourgois, G., Colom, P., & Crovisier, J. 1987, A&A, 187, 455
Gérard, E., Bockelée-Morvan, D., Bourgois, G., Colom, P., & Crovisier, J. 1988, A&AS, 74, 485
Gérard, E., Bockelée-Morvan, D., Bourgois, G., Colom, P., & Crovisier, J. 1989, A&AS, 77, 379
Gérard, E., Bockelée-Morvan, D., Colom, P., & Crovisier, J. 1993, in Astrophysical Masers, ed. A. W. Clegg, & J. E. Nedoluha, Lectures Notes in Physics 412 (Springer-Verlag), 468
Gérard, E., Crovisier, J., Colom, P., et al. 1998, Planet. Space Sci., 46, 569
Gérard, E., & Drouhin, J. P. 1984, IAU Circ., 3967
IHW Archive, 1992
Jorda, L. 1995, Atmosphères cométaires: Interprétation des Observations dans le Visible et Comparaison avec les Observations Radio, Thesis, Université Paris VII
Jorda, L., Crovisier, J., & Green, D. W. E. 1992, in Asteroids Comets Meteors 1991, ed. A. W. Harris, & E. Bowell, 285
Jorda, L., Crovisier, J., & Green, D. W. E. 1996, preprint
Jorda, L., & Rickman, H. 1995, Planet. Space Sci., 43, 575
Mäkinen, J. T. T., Bertaux, J.-L., Pulkkinen, T. I., et al. 2001a, A&A, 368, 292
Mäkinen, J. T. T., Silén, J., Schmidt, W., et al. 2001b, Icarus, 152, 268
Mies, F. H. 1974, ApJ, 191, L145
Mies, F. H. 1976, in The Study of Comets, ed. B. Donn, M. Mumma, W. Jackson, M. A'Hear, & R. Harrington, NASA SP-393, 843
Palmer, P., de Pater, I., & Snyder, L. R. 1989, AJ, 97, 1791
Reich, P., & Reich, W. 1986, A&AS, 63, 205
Rickman, H., & Jorda, L. 1998, Adv. Space Sci., 21(11), 1491
Rydbeck, O. E. H., Ellder, J., Ronnang, B., et al. 1974, Icarus, 23, 595
Schenewerk, M. S., Palmer, P., Snyder, L. E., & de Pater, I. 1986, AJ, 92, 166
Schleicher, D. G., & A'Hearn, M. F. 1988, ApJ, 331, 1058
Schloerb, F. P. 1988, ApJ, 332, 524
Schloerb, F. P., Claussen, M. J., & Tacconi-Garman, L. 1987, A&A, 187, 469
Schloerb, F. P., Devries, C. H., Lovell, A. J., et al. 1999, Earth Moon Planets, 78, 45
Stern, S. A., Parker, J. W., Festou, M. C., et al. 1998, A&A, 335, L30
Tacconi-Garman, L. E., Schloerb, F. P., & Claussen, M. J. 1990, ApJ, 364, 672
Turner, B. 1974, ApJ, 189, L137
van Driel, W., Pezzani, J., & Gérard, E. 1996, in High Sensitivity Radio Astronomy, ed. N. Jackson, & R. J. Davis (Cambridge Univ. Press, Cambridge, UK), 229
Webber, J. C., & Snyder, L. E. 1977, ApJ, 214, L45
Xie, X. 1994, Cometary Atmospheres: Monte Carlo Simulation and its Application to OH Radio Observations, Ph.D. dissertation, University of Pensylvania